Received: 15 June 2022 | Revised: 18 December 2022 | Accepted: 19 December 2022

DOI: 10.1111/gcb.16582

Global Change Biology WILEY

RESEARCH ARTICLE

The ecosystem wilting point defines drought response and recovery of a *Quercus-Carya* forest

Jeffrey D. Wood[1] | Lianhong Gu[2] | Paul J. Hanson[2] | Christian Frankenberg[3,4] | Lawren Sack[5]

[1]School of Natural Resources, University of Missouri, Columbia, Missouri, USA

[2]Environmental Sciences Division and Climate Change Institute, Oak Ridge National Laboratory, Oak Ridge, Tennessee, USA

[3]Division of Geological and Planetary Sciences, California Institute of Technology, Pasadena, California, USA

[4]Jet Propulsion Laboratory, California Institute of Technology, Pasadena, California, USA

[5]Department of Ecology and Evolutionary Biology, University of California, Los Angeles, Los Angeles, California, USA

Correspondence
Jeffrey D. Wood, School of Natural Resources, University of Missouri, Columbia, MO, USA.
Email: woodjd@missouri.edu

Funding information
U.S. Department of Energy, Office of Science, Office of Biological and Environmental Research; ORNL is managed by UT-Battelle, LLC, for the DOE under contract, Grant/Award Number: DE-AC05-00OR22725; National Science Foundation, Grant/Award Number: 2017949

Abstract

Soil and atmospheric droughts increasingly threaten plant survival and productivity around the world. Yet, conceptual gaps constrain our ability to predict ecosystem-scale drought impacts under climate change. Here, we introduce the ecosystem wilting point (Ψ_{EWP}), a property that integrates the drought response of an ecosystem's plant community across the soil–plant–atmosphere continuum. Specifically, Ψ_{EWP} defines a threshold below which the capacity of the root system to extract soil water and the ability of the leaves to maintain stomatal function are strongly diminished. We combined ecosystem flux and leaf water potential measurements to derive the Ψ_{EWP} of a *Quercus-Carya* forest from an "ecosystem pressure–volume (PV) curve," which is analogous to the tissue-level technique. When community predawn leaf water potential (Ψ_{pd}) was above Ψ_{EWP} (=−2.0 MPa), the forest was highly responsive to environmental dynamics. When Ψ_{pd} fell below Ψ_{EWP}, the forest became insensitive to environmental variation and was a net source of carbon dioxide for nearly 2 months. Thus, Ψ_{EWP} is a threshold defining marked shifts in ecosystem functional state. Though there was rainfall-induced recovery of ecosystem gas exchange following soaking rains, a legacy of structural and physiological damage inhibited canopy photosynthetic capacity. Although over 16 growing seasons, only 10% of Ψ_{pd} observations fell below Ψ_{EWP}, the forest is commonly only 2–4 weeks of intense drought away from reaching Ψ_{EWP}, and thus highly reliant on frequent rainfall to replenish the soil water supply. We propose, based on a bottom-up analysis of root density profiles and soil moisture characteristic curves, that soil water acquisition capacity is the major determinant of Ψ_{EWP}, and species in an ecosystem require compatible leaf-level traits such as turgor loss point so that leaf wilting is coordinated with the inability to extract further water from the soil.

KEYWORDS
ecosystem fluxes, ecosystem trait, eddy covariance, predawn leaf water potential, turgor loss point

1 | INTRODUCTION

Drought has major impacts on natural resources, food, water, and socioeconomic systems (Pulwarty & Sivakumar, 2014) and is a primary factor limiting global vegetation productivity (Gampe et al., 2021; Liu, Zhou, et al., 2021; Madani et al., 2020; Stocker et al., 2019; Zhang et al., 2022). Drought is projected to increase in frequency and intensity during the 21st century; thus, agricultural and natural ecosystems are likely to face intensifying water stress (Zhao & Dai, 2022). Understanding ecosystem functional responses to drought is crucial for accurately predicting changes in climate and the carbon cycle (Novick et al., 2016; Paschalis et al., 2020) and for developing strategies for risk management. Plant responses to both soil water deficit and atmospheric vapor pressure deficit (VPD), individually and in combination, determine ecosystem-level drought responses (Grossiord et al., 2020; Liu, Gudmundsson, et al., 2020; Lansu et al., 2020; Novick et al., 2016; Stocker et al., 2018; Zhang et al., 2019). Yet, scaling up drought responses from organs/tissues and whole plants to ecosystems is challenging because of scale emergent behavior at higher levels of biological organization (Anderegg et al., 2018; Liu, Holtzman, et al., 2021), complicating the linking of traditional plant functional traits with whole-ecosystem function.

At the plant scale, drought response thresholds for many functions have been well characterized, with the leaf turgor loss point (Ψ_{tlp}) being one such key threshold. When stomata open to enable carbon dioxide (CO_2) uptake, evaporative water loss from the mesophyll causes leaf water potential (Ψ_{leaf}) to decline and tensions to develop throughout the plant hydraulic system (Melvin T. Tyree & Zimmermann, 2002). If the transpiration stream cannot match evaporative demand, leaves dehydrate, and declining turgor pressure induces stomatal closure, restricting gaseous diffusion into and out of the leaf (Bartlett et al., 2014). Eventually, when Ψ_{leaf} reaches the Ψ_{tlp} (i.e., the wilting point), turgor pressure is zero and the total Ψ_{leaf} is equal to the osmotic potential—past this point, any decline in Ψ_{leaf} corresponds directly to leaf cell volume shrinkage (Sack et al., 2018). To maintain Ψ_{leaf} safely above Ψ_{tlp}, plants often coordinate traits across the soil–plant–atmosphere continuum (SPAC) to mediate water use, and balance water supply and demand (Flo et al., 2021; Lu et al., 2020; McCulloh et al., 2019; Scoffoni et al., 2016). Ψ_{tlp} is thus a key drought tolerance trait that often correlates with climatic aridity across species and biomes (Bartlett et al., 2012, 2014, although see Farrell et al. 2017).

Early research on plant wilting, motivated by the desire to understand field water budgets for crop management purposes, led to the concept of the soil "permanent wilting point" (PWP; Briggs & Shantz, 1912; Kirkham, 2005; Richards & Weaver, 1943; Veihmeyer & Hendrickson, 1928). Note that the "permanent" in PWP was defined in the context of drought experiments, and it corresponds to the point at which plants that wilted during the day under a hot sun would no longer recover overnight upon equilibration with the soil. Yet, "permanent" is just in the sense of experimental drought conditions; while they remained alive, the plants could recover from wilting when re-watered. Early studies focused on crops in well-watered systems led to the notion that plants wilted at similar soil matric potentials, and the approximate definition of the PWP as the water content held at a soil matric potential of −1.5 MPa became widely adopted in soil science (Kirkham, 2005; Tolk, 2003).

Meanwhile, plant physiologists developed understanding of cellular (Höfler, 1920), tissue, and organ water relations (Richter, 1978; Scholander et al., 1964; Tyree & Hammel, 1972). Over decades, considerable variability, and a wide range of turgor loss points (Bartlett et al., 2012), as well as "wilting points" for plants grown under different soil textures have been observed (Kursar et al., 2005; Wiecheteck et al., 2020). The wilting point of the bulk leaf is defined by the water potential at the turgor loss point (Pallardy et al., 1991). Leaf Ψ_{tlp} varies considerably across plant species (Bartlett et al., 2012), and is strongly correlated with other drought response thresholds of the hydraulic, stomatal, and photosynthetic systems (Bartlett et al., 2016). Furthermore, the turgor loss point often displays plasticity due to osmotic adjustment—in other words for a given plant growing in a given soil, leaf Ψ_{tlp} can change over time, reinforcing that a universal wilting point should not be expected (Bartlett et al., 2014). Given that stomata close at the turgor loss point, transpiration is reduced to a small fraction of the well-watered rate, and only minimal transpiration-driven tension can be generated by the plant; thus, plant water potentials remain close to equilibrated with the soil, and thus, in principle, Ψ_{tlp} represents the soil water potential below which water extraction by the plant is not possible (Bartlett et al., 2012).

Despite recognition of Ψ_{tlp} as a physiological determinant of plant drought performance, the concept has not been scaled up to the ecosystem level for understanding dynamic environmental responses and biogeography. Traditionally, ecosystem-level analyses have tended to focus on photosynthetic carbon gain and water loss rates in direct relationship with environmental variables, without a consideration of internal plant water status, which integrates environmental responses (Baldocchi, 2020; Novick et al., 2022; Reichstein et al., 2014). In general, ecosystem traits related to maximal carbon and water fluxes such as leaf area index (LAI) or light-saturated GPP can explain variation in function among ecosystems across climatic gradients, and there have been proposals to develop additional integrated ecosystem traits based on plant traits expressed at the community level (He et al., 2019; Reichstein et al., 2014).

Progress from the standpoint of ecosystem water relations traits has, however, been slower to develop, with recent model-data fusion examples at the scale of ecosystems (Liu, Kumar, et al., 2020) and remote sensing grid cells, that is, 0.25° grid cells (Liu, Holtzman, et al., 2021; Liu, Konings, et al., 2021). In all these cases, a prescribed model is used as a framework for retrieving a suite of bulk traits that result in the model best matching observed constraints such as ecosystem fluxes (Liu, Kumar, et al., 2020) or remotely sensed data like vegetation optical depth (Liu, Holtzman, et al., 2021; Liu, Konings, et al., 2021). Scaling up from organs/traits to ecosystems and larger scales can be complicated by scale emergent behavior at higher levels of organization (Baldocchi et al., 2021; Liu, Konings, et al., 2021;

Reichstein et al., 2014) and is particularly relevant for advancing macroecological understanding of water relations and Earth system modeling.

A recent review proposed that an ecosystem analog of the pressure–volume (PV) curve would be useful for relating remotely sensed vegetation water content to water potential, and parameters that can be extracted from such a curve (e.g., an ecosystem wilting point) might have macroecological applications (Konings et al., 2021). Here, we develop a novel "top-down" method that synthesizes ecosystem flux and predawn Ψ_{leaf} observations to determine an ecosystem analog to Ψ_{tlp} that we call the "ecosystem wilting point" (Ψ_{EWP}). The Ψ_{EWP} is an ecosystem trait that integrates canopy behavior with both climate and soil properties and represents the point below which the extraction of soil water by the root system is extremely challenging, and leaves are at, or very near Ψ_{tlp}. We hypothesize Ψ_{EWP} is strongly constrained by the capacity for soil water acquisition by vegetation, which is jointly determined by the root density distribution and the soil moisture characteristic (i.e., water retention curve).

We tested how Ψ_{EWP} relates to gas exchange dynamics, hypothesizing that Ψ_{EWP} is a functional threshold defining a transition in the responsiveness of vegetation to environmental dynamics. We also tested the influence of community predawn leaf water potential (Ψ_{pd}) declining below Ψ_{EWP} on ecosystem light use efficiency (LUE) and ecosystem intrinsic water-use efficiency (iWUE). We hypothesized divergent LUE and iWUE responses, with LUE showing immediate declines with the onset of mild-to-moderate stress owing to stomatal regulation of GPP. In angiosperms, the leaf-level stomatal conductance (g_s) of well-watered plants exceeds what is needed for maximizing leaf iWUE; under drought stress, plants downregulate g_s and increase leaf-level iWUE (Yang et al., 2021). We thus hypothesized that ecosystem iWUE also increases under mild-to-moderate drought stress until the ecosystem reaches Ψ_{EWP}, at which point vegetation reduces g_s at the expense of optimizing carbon gain, and thus ecosystem iWUE declines.

2 | METHODS

2.1 | Site description and observations

The Missouri Ozark AmeriFlux (MOFLUX) site (ID: US-MOz; lat. 38.7441°, long. −92.2000°) is situated in the Ozark Border Region at the University of Missouri's Baskett Forest (Gu et al., 2015; Gu, Pallardy, Yang, et al., 2016; Yang et al., 2010). The site is a second-growth, *Quercus-Carya* (oak-hickory) forest, with important tree species including *Quercus alba* L. (white oak), *Quercus velutina* Lam. (black oak), *Carya ovata* (Mill.) K. Koch. (shagbark hickory), *Acer saccharum* Marsh. (sugar maple), and *Juniperus virginiana* L. (eastern redcedar), with *Fraxinus americana* L. (white ash) scattered throughout the site. The dominant soils are Weller silt loam (fine, smectic, mesic Aquertic Chromic Hapludalf) and Clinkenbeard very flaggy clay loam (clayey-skeletal, mixed, superactive, mesic Typic Argiudoll) underlain by Ordovician and Mississippian limestones. Total root densities decline from a maximum of around 5.5 kg m^{-3} in the upper 22 cm of soil to approximately 0.2 kg m^{-3} at the 60–72 cm depth, while the densities of roots with diameter <3 mm were approximately 2.5 kg m^{-3} and 0.1 kg m^{-3} in the 0–22 cm and 60–72 cm layers, respectively (Figure S1). The mean annual air temperature and precipitation are 12.5°C and 1052 mm, respectively (1991–2020 climate normals; Columbia Regional Airport; station USW00003945; https://www.ncei.noaa.gov/products/us-climate-normals).

Detailed descriptions of the micrometeorological instrumentation and calculations are available in the literature (Gu et al., 2012; Gu, Pallardy, Yang, et al., 2016; Liu, Liang, et al., 2020). Briefly, net ecosystem exchanges of CO_2 (NEE), water vapor, and sensible heat (H) were measured using eddy covariance. The eddy covariance systems were deployed on a 32 m scaffold tower, on which profile measurements (CO_2, water vapor, and air temperature) were also made to estimate the effective change in storage. Soil respiration (R_s) was measured using an automated chamber system (model LI-8100A, Li-Cor Inc., Lincoln, NE, USA) configured with 16 chambers. Ecosystem flux and supporting meteorological observations were recorded at half-hourly resolution. The soil respiration system measured each chamber once per hour, which were used to compute hourly means that were interpolated to half-hourly values to match the temporal resolution of ecosystem fluxes (Liu, Liang, et al., 2020).

Net ecosystem fluxes were calculated as the sum of the eddy flux and effective change in storage and have a negative sign when directed from the atmosphere to the ecosystem (Gu et al., 2012). An objective friction velocity filtering approach was used to screen out NEE of CO_2 data during nighttime periods with poorly developed turbulence (Gu et al., 2005); gaps were filled using the mean diurnal variation approach (Falge et al., 2001).

Gross primary productivity (GPP, positive values represent CO_2 uptake) was calculated according to $\mathrm{GPP} = R_S - \mathrm{NEE}$ (Yang et al., 2010). For validation purposes, we compared the R_S-based GPP to estimates derived from the so-called "nighttime" and "daytime" methods (see supplementary methods, "Inferring GPP—methods comparison" and Figure S2).

Surface conductance (G_S) was computed by inverting the Penman–Monteith equation (Novick et al., 2016; Zhang et al., 2006):

$$\frac{1}{G_S} = \frac{\rho c_p D}{\gamma \bullet LE} + \frac{(Bs/\gamma) - 1}{G_a} \quad (1)$$

where LE is the latent heat flux (W m^{-2}), ρ the air density (kg m^{-3}), c_p the specific heat capacity of air (J kg^{-1} K^{-1}), D the VPD of the air (kPa), B the Bowen ratio, s the slope of the saturation vapor pressure curve (kPa K^{-1}), γ is the psychrometric constant (kPa K^{-1}), and G_a the aerodynamic conductance. G_a was calculated according to $G_a^{-1} = u \bullet u_*^{-2} + 6.2 \bullet u_*^{-0.67}$, where u and u_* the mean horizontal wind speed (m s^{-1}) and friction velocity (m s^{-1}), respectively (Monteith & Unsworth, 1990).

Predawn leaf water potential was measured at weekly to biweekly intervals (Gu et al., 2015). Samples (N = 20–21) from individuals comprising the major species were collected before dawn in

rough proportion to their relative basal area contributions. Samples excised from lower branches (<2 m) were placed in humidified bags, and stored in a cooler on ice until analysis using the pressure chamber technique (Pallardy et al., 1991). The community predawn leaf water potential (Ψ_{pd}) was computed as the arithmetic mean of samples collected on a given day because of the proportional species sampling strategy.

Ecosystem LUE (mol C mol^{-1} photons) was computed as the ratio of GPP to ecosystem absorbed photosynthetically active radiation (APAR, μmol m^{-2} s^{-1}), which was approximated as the difference between incoming and outgoing PAR measured at the top of the canopy. Ecosystem iWUE (μmol-C mol^{-1} H_2O) was taken as the ratio of GPP to G_S. For examining annual cycles of LUE and iWUE, we computed mean values for each day for conditions of high light (solar irradiance >500 W m^{-2}) between 1000 and 1500 h local standard time.

In this work, we primarily focus on observations made during the exceptional drought year of 2012, with some comparisons to wet-year conditions for context. Wet-year conditions were determined for the 2 years with the least negative predawn leaf water potential integrals, that is, water stress integrals (Myers, 1988).

2.2 | Analyses

2.2.1 | Ecosystem PV analysis

We conducted a whole-ecosystem PV analysis, where we consider the entire soil vegetation system. Much like how PV analysis arose from scaling up cell-level concepts to tissues or organs (Tyree & Hammel, 1972), with extension to ecological applications (Bartlett et al., 2012, 2014; Cheung et al., 1975), the jump from organ to ecosystem scale is inevitable (Konings et al., 2021). Just as the leaf PV curve "bulks" all the cells and tissues, the ecosystem analysis further "bulks" the cells and tissues of all the trees of all species together, as well as the volume of available soil water. From the ecosystem PV analysis (described below), we derive Ψ_{pd} at the *ecosystem wilting point* (Ψ_{EWP}). Ψ_{EWP} integrates aboveground and belowground plant traits and environmental responses that together define the ability of vegetation to balance water acquisition from soils, and the capacity of leaves to maintain turgor and gas exchange. When Ψ_{pd} falls below Ψ_{EWP}, the canopy gas exchange is significantly inhibited and unable to respond to environmental dynamics.

Our ecosystem PV approach blends two classic techniques from plant water relations—the "squeeze" (Scholander et al., 1964) and "bench drying" (Richter, 1978) methods. Both methods require serial measurements of tissue water potential as a sample is dehydrated from a state of full hydration (Pallardy et al., 1991). The "bench drying" method involves bench drying a sample and measuring changes in the tissue water potential and mass over a substantial period of time (i.e., >24 h). In the "squeeze" method, the sample is in a pressure chamber, and as the pressure is slowly increased, the volume of sap expressed from the sample is determined. Our ecosystem-scale approach is analogous to the "bench-dry" method in that natural dehydration decreases water potentials, and like the "squeeze" approach in that we quantify the cumulative volume (mass) of water lost through ET.

We analyzed measurements of Ψ_{pd} and ET during the 2012 drought. We used Ψ_{pd} for both practical (mid-day Ψ_{leaf} measurements were not made) and theoretical reasons. Theoretically, for the purposes of defining a whole-ecosystem wilting point that links soil characteristics with plant structural and functional traits, Ψ_{pd} is superior to mid-day Ψ_{leaf}. First, Ψ_{pd} better represents whole-ecosystem water status because at predawn, water throughout the SPAC is close to equilibrium. In other words, leaf water is at or close to equilibrium with water in the soil volume that is being explored by roots, and as such, sometimes Ψ_{pd} is used as a proxy for soil water potential (Pallardy et al., 1991). In contrast, because of high daytime transpiration rates, water in the SPAC is in disequilibrium and there are strong mid-day Ψ_{leaf} gradients through the canopy depth (and all are below soil water potential). Furthermore, short-term variations in atmospheric conditions (e.g., solar irradiance, VPD) can induce rapid fluctuations in Ψ_{leaf}. Moreover, Ψ_{pd} represents the maximum water availability for the given day, to which plants are sensitive for growth. Therefore, Ψ_{pd} is a better integrated metric of ecosystem water status for relating to cumulative ET.

Using 2012 data, we calculated cumulative ET from DOY 136—the first day Ψ_{pd} was measured—through DOY 243, the last day that Ψ_{pd} was observed before re-wetting by soaking rains. Daily ET was normalized by LAI to account for drought-induced leaf abscission. Although the 2012 drought event was very intense, there was scattered precipitation during the dry-down (Figure 1a,b). If daily rainfall was ≤5 mm, we subtracted the daily rainfall from ET for that day, setting any negative values to 0. If daily rainfall was >5 mm, we set ET to zero on that day, and we subtracted 5 mm from ET on the next day. At this site, 5 mm of rain is the amount required to fully wet the canopy and litter such that there is wetting of the mineral soil that can improve maintenance of the transpiration stream (Gu, Pallardy, Hosman, et al., 2016). We did not include two Ψ_{pd} observations in the analyses that were associated with short-lived rebounds of Ψ_{pd} values immediately following small rainfall events. We re-calculated Ψ_{EWP} without the above-described rainfall-based screening of ET and it did not alter our findings.

PV curve analysis involves analyzing a plot of reciprocal water potential (i.e., $-1/\Psi$) versus relative water content or cumulative sap expression, which yields a biphasic, monotonically decreasing function. The turgor loss point is the water potential at the change point between the first strong nonlinear, and second less-sensitive linear decreasing phases (Pallardy et al., 1991). The nonlinearity of the first phase arises due to simultaneous declines in both turgor and osmotic potentials, while the second, less-sensitive linear phase corresponds strictly to increasing osmotic concentrations (i.e., declining osmotic potential) as cell volumes decline (Sack et al., 2018). In our ecosystem-scale analysis, we expected and subsequently found a response comprised of two linear segments separated by a change point that corresponds to Ψ_{EWP}. We

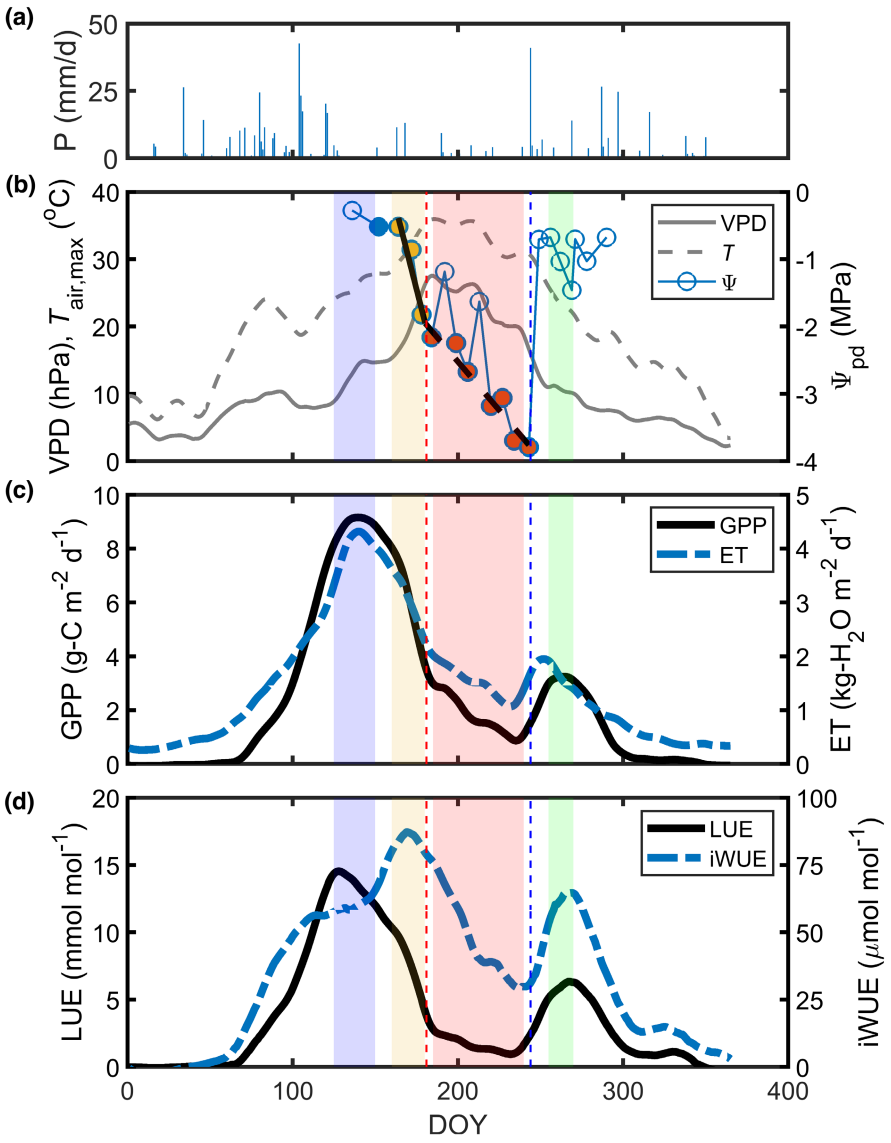

FIGURE 1 Time series of (a) daily precipitation, (b) daytime mean atmospheric vapor pressure deficit (VPD), daily maximum air temperature ($T_{air,max}$) and community predawn leaf water potential (Ψ_{pd}), (c) daily gross primary productivity (GPP), daily evapotranspiration (ET), and (d) mid-day light use efficiency (LUE) and intrinsic water use efficiency (iWUE). All time series except Ψ_{pd} were smoothed; the vertical dashed red and blue lines correspond to when Ψ_{pd} fell below the ecosystem wilting point, and the soaking rains that provided drought relief, respectively. In (a), the solid and dashed black lines are from a two-phase linear fit to the Ψ_{pd} time series. The shaded periods correspond to peak flux (blue), flash stress (yellow), wilted (red) and recovery (green) periods referenced in Table S1, and Figures S6–S8, which show corresponding mean daily cycles, and responses to light and VPD, respectively.

fitted a biphasic linear regression to the observations to determine Ψ_{EWP} (see supplementary methods, "Biphasic linear regression analysis").

Leaf PV curves may have an initial plateau when the tissues are fully turgid owing to the presence of liquid water in intercellular air spaces (Pallardy et al., 1991; Parker & Pallardy, 1987). We expected that the ecosystem PV curve would have an initial plateau corresponding to the period when plant available water is readily extracted from soils and vegetation is not subject to significant water stress. Plateaus do not affect the determination of Ψ_{tlp} in tissue-level analyses (Abrams & Menges, 1992), and thus we did not remove it before statistical analysis, though we only fit the biphasic linear regression model to data that contained the dry down signal where $-1/\Psi_{pd}$ declined strongly with increasing cumulative ET.

To place our Ψ_{EWP} estimate in context, we compared it to the distribution of weekly to bi-weekly Ψ_{pd} observations (N = 280) derived from >5500 species-level predawn Ψ_{leaf} measurements made over a 16-year period (2005–2020).

2.2.2 | Soil and root trait analyses

We conducted analyses to test how belowground traits that influence the ability of vegetation to acquire water from the soil may constrain Ψ_{EWP}. We used soil moisture characteristic curves to determine soil water potential thresholds that define a regime shift to a situation where it is exceedingly difficult for roots to extract soil water, hypothesizing that the root system becomes tuned to these thresholds. These thresholds correspond to change points in the soil moisture characteristic curves where the volumetric water content became virtually invariant with further declines in soil water potential. We then used the root density profiles to calculate a weighting function. Integrating the product of the root density weighting function and water potential threshold function across the root zone yielded a single value for the soil-based wilting point of the ecosystem, $\Psi_{EWP,soil}$. The theory, methods, and data used for these analyses are described in more detail in the supplementary methods ("Soil and root trait analysis methods").

3 | RESULTS

Year 2012 was hot and dry (Figure 1a,b; supplementary results "Annual cycles"; Figures S3–S5). Notably, elevated VPD and low soil water supply modulated the annual cycles of ecosystem gas exchange and resource use efficiencies, giving each a "dual peak" signature, with the second peaks associated with a recovery period following soaking rains (Figure 1). The first signs of mild to moderate water stress were observed shortly after the spring peaks of GPP and ET when Ψ_{pd} declined to approximately −0.5 MPa, where it held for just under 2 weeks, after which there was a strong biphasic drydown characterized by fast and then slow linear declines in Ψ_{pd} over time (Figure 1b). The fast Ψ_{pd} decline lasted about 2 weeks, during which time Ψ_{pd} dropped to approximately −2 MPa, while the ensuing slow Ψ_{pd} decline lasted 2 months.

3.1 | The ecosystem PV curve and wilting point

The ecosystem PV curve had a "plateau" where cumulative ET increased without a change in $-1/\Psi_{pd}$ (Figure 2). During this initial stable period, ET rates were high as the vegetation readily extracted soil water. When cumulative ET reached ~27 kg-H_2O m^{-2} leaf, the PV curve displayed biphasic, monotonically decreasing behavior, with an initial steep phase, followed by a second characterized by a gentler slope. The change point between the two phases defines Ψ_{EWP}, which was −2.0 (95% CI; −2.23, −1.78) MPa for this forest.

We conducted a "bottom-up" analysis based on the water retention characteristics of the soils and the root density distribution to estimate the ecosystem wilting point based on the root density distribution and the point at which further soil water extraction is exceedingly difficult through analysis of soil moisture characteristic curves (Figure 3). This trait-based analysis yielded a soil-based ecosystem wilting point ($\Psi_{EWP,soil}$) of −2.0 (−3.12, −1.16) MPa, identical to our "top-down" ecosystem PV analysis estimate of Ψ_{EWP}, albeit with wider uncertainty bounds.

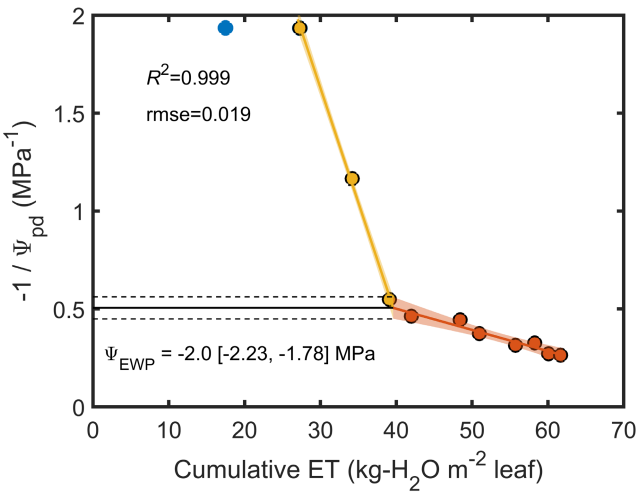

FIGURE 2 Ecosystem pressure–volume (PV) curve analysis, showing the results of the two-phase regression (yellow and red lines). Cumulative ET was calculated starting the day of the first predawn leaf water potential (Ψ_{pd}) observation in 2012. The Ψ_{pd} at the wilting point, Ψ_{EWP}, was −2.0 (−2.23, −1.78) MPa, where the values in brackets denote the 95% confidence interval. The symbol fill and line colors map Ψ_{pd} observations to the time series plot in Figure 1a.

From 2005 through 2020, 10% and 59% of Ψ_{pd} observations (N = 280) were below Ψ_{EWP} and −0.5 MPa, respectively (Figure 4). Thus, about half of the observations fell between Ψ_{pd} of −0.5 MPa and Ψ_{EWP}. When Ψ_{pd} reaches −0.5 MPa, this forest is in a precarious position and without soaking rains it can enter into precipitous Ψ_{pd} decline within about 2 weeks, and could reach Ψ_{EWP} in another 2 weeks (Figure 1b). Taken together, during the growing season, this forest often functions in a state whereby very hot/dry periods of 2–4 weeks can quickly result in intense physiological drought stress.

3.2 | The ecosystem wilting point as a functional threshold

We analyzed data during the strong downregulation of ecosystem fluxes and found that the Ψ_{EWP} is a threshold defining marked shifts in ecosystem functional state (Figure 5). The change point in the Ψ_{pd} time series corresponding to when Ψ_{pd} fell below Ψ_{EWP} was highly coherent with change points in the time series of daily GPP, daily ET, and mid-day means of GPP, G_S, LUE, and iWUE. For all variables except iWUE, the change points corresponded to shifts from fast to slow rates of decline over time. In contrast, iWUE increased through moderate drought stress, with the change point corresponding to peak observed values and a transition to declining iWUE around the time of ecosystem wilting. Moreover, an examination of daily flux dynamics underscored how the forest's ability to respond to environmental variations (e.g., VPD and light) became strongly diminished when Ψ_{pd} fell below Ψ_{EWP} (Figure 6 and Figures S6 and S8; supplementary text, Results: Daily flux dynamics).

3.3 | Recovery from drought

Soaking rains at the end of August caused rapid leaf rehydration (Figure 1a,b) and resumption of ET (some of which was from surface evaporation), while GPP and NEE lagged behind (Figures 1c and 7). Leaf rehydration to Ψ_{pd} values above Ψ_{EWP} occurred within 6 days, though this estimate was constrained by the timing of sampling relative to the rainfall. Peak GPP recovery lagged the rainfall event by about 2 weeks.

NEE recovered to values consistent with wet years for the same time of year (Figure 7a), which is particularly notable given that intense drought conditions flipped the forest to a net CO_2 source for almost every day in July and August. In contrast, GPP, R_S, and ET did not recover to values consistent with wet years (Figure 7b–d). During drought recovery, GPP was about half that of the corresponding wet reference year (Figure 7b) due to a combination of structural (e.g.,

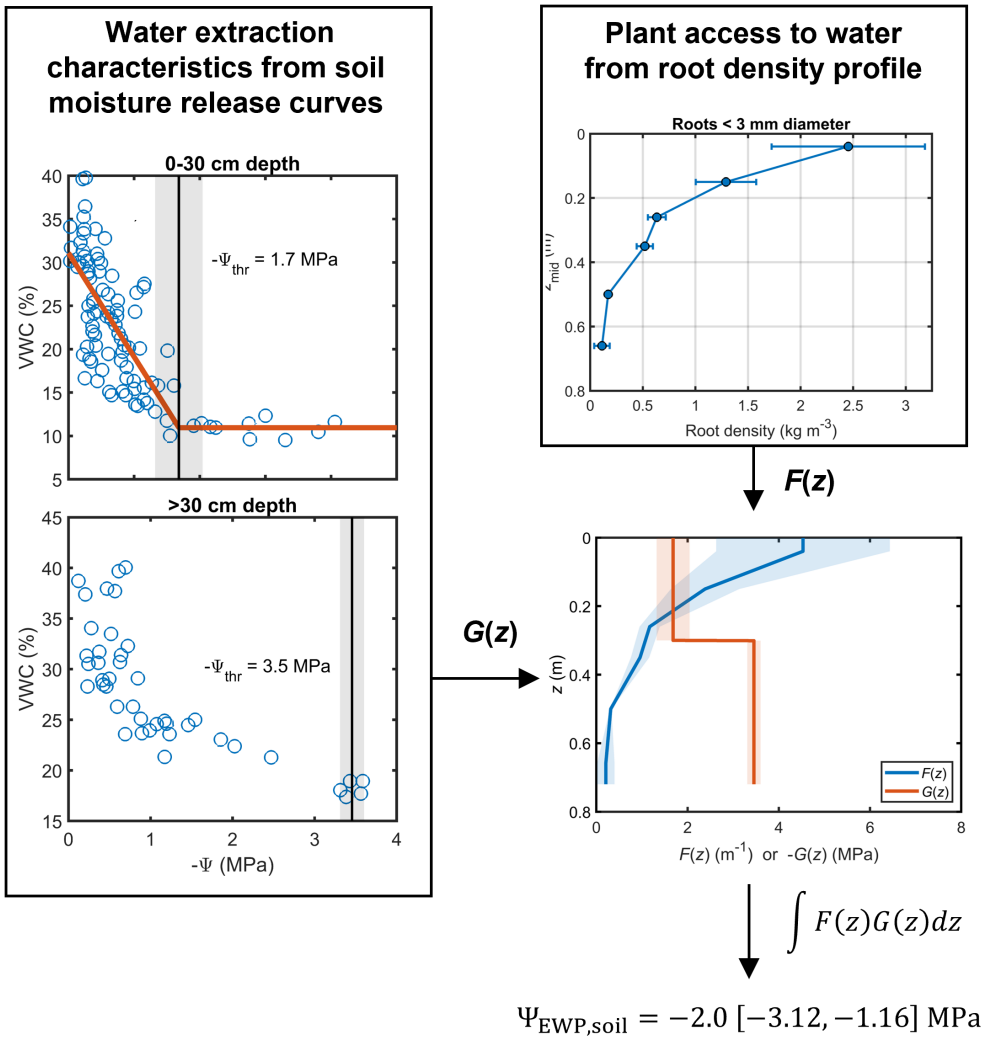

FIGURE 3 Estimation of ecosystem wilting point from soil moisture release characteristics and the root density distribution ($\Psi_{EWP,soil}$). Water extraction characteristics from soil moisture release curves were combined with a root density distribution function that represents the vegetation's access to the profile. The capacity for water extraction was defined by a water potential threshold (Ψ_{thr}), which separates the moisture characteristics into two broad regions of water accessibility.

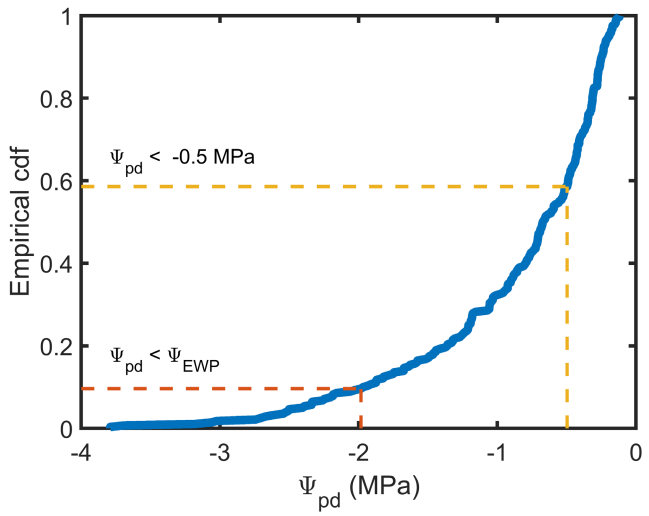

FIGURE 4 Empirical cumulative distribution function of community predawn leaf water potential (Ψ_{pd}) observed from 2005 through 2020 ($N = 280$). Ψ_{EWP}, ecosystem wilting point.

leaf abscission, Figure S3f) and physiological damage. Indeed, photosynthetic capacity as inferred from light-saturated GPP recovered to values that were about half of those during the same time period during wet years (Figure 6a vs. Figure S7a). It should, however, be noted that recovery to a functional state similar to the early season was not expected because of declining maximum daytime PAR and daylengths, and the associated phenological transition.

Both iWUE and LUE also showed rapid recovery in response to wetting; however, the timing of recovery peaks lagged the fluxes (Figure 1d vs. Figure 1c). For context, we compared the annual cycles of the drought year to wet reference conditions (Figure 8). At peak recovery, LUE was ~50% lower than corresponding values during wet conditions, while iWUE was ~85% higher than the wet reference. Though there was strong functional recovery after rainfall, vegetation was still experiencing water stress as evidenced by the peak Ψ_{pd} recovery values of about −0.7 MPa (Figure 1b; Table S1). Moreover, by the end of the drought, there was necrosis of leaf tissue in the uppermost exposed canopy layer (Kravitz et al., 2016) that presented

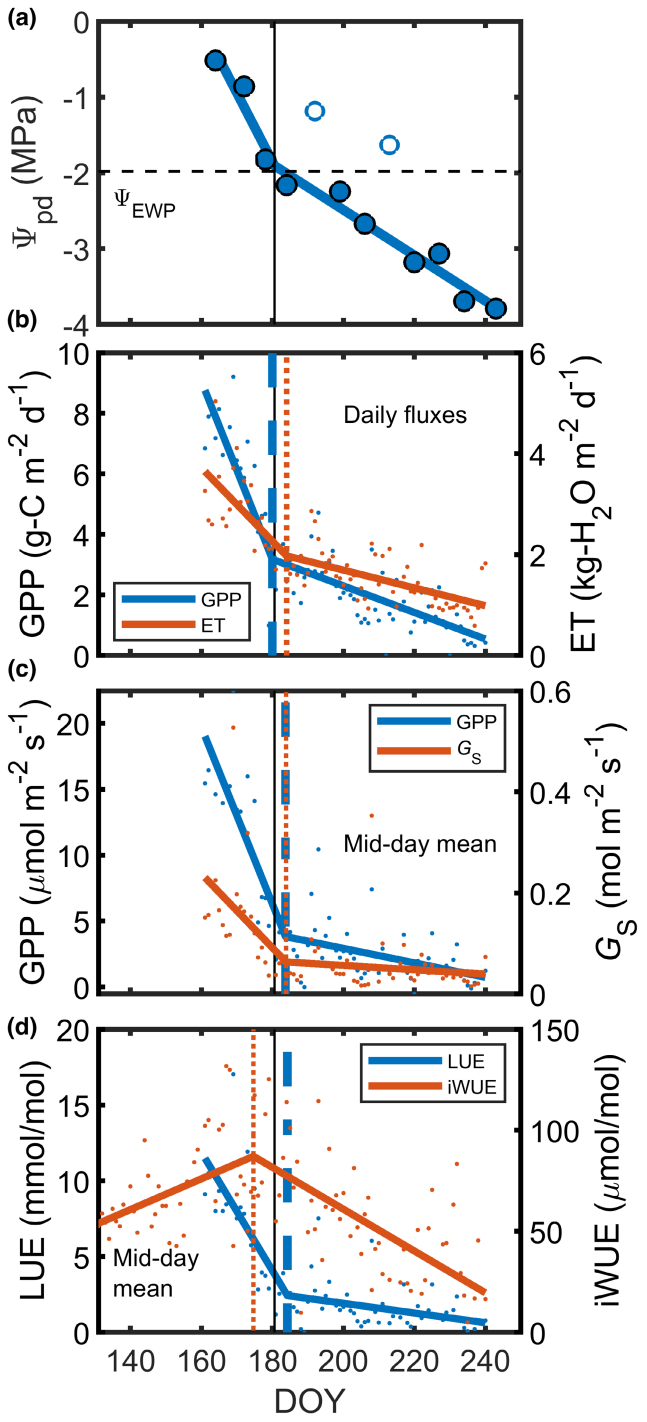

FIGURE 5 The ecosystem wilting point (Ψ_{EWP}) defines marked shifts in ecosystem functional state. There were highly coherent change points in the time series of (a) Ψ_{pd} (un-filled symbols represent transient responses to small rainfall events that were not included in the regression), (b) daily GPP and ET, (c) mid-day mean GPP and G_S, and (d) mid-day LUE and iWUE. Vertical black reference lines indicate the change point in the Ψ_{pd} time series. Vertical dashed blue and dotted red reference lines denote the change points of the data with the matching colors. A different date range was used for the iWUE analysis because it behaved differently than all other variables. ET, evapotranspiration; GPP, gross primary productivity; G_S, surface conductance; LUE, light use efficiency; iWUE, ecosystem intrinsic water use efficiency; Ψ_{pd}, community predawn leaf water potential.

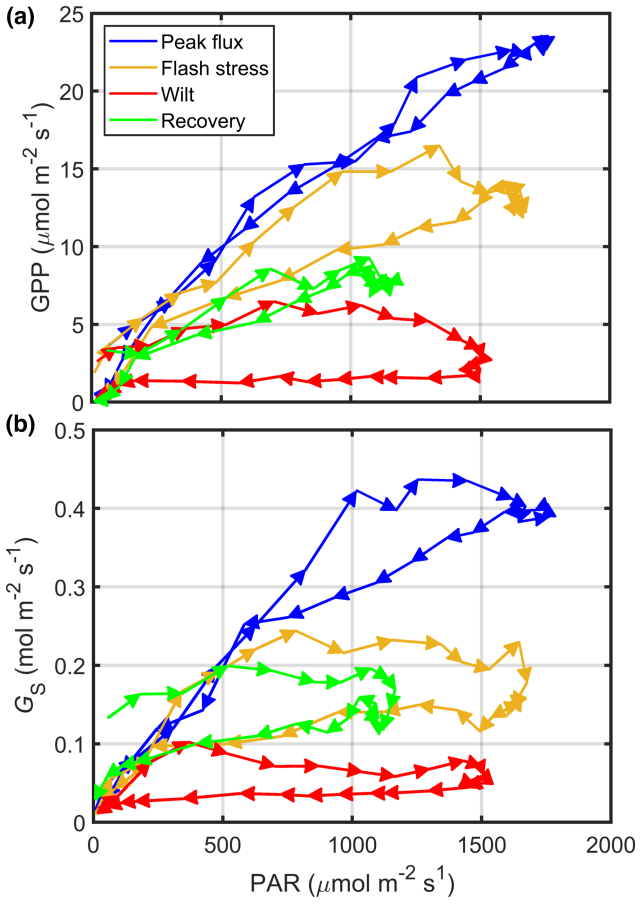

FIGURE 6 (a) Gross primary productivity (GPP) and (b) surface conductance (G_S) became insensitive to light and showed greater hysteresis as drought intensified, and the ecosystem wilted. The progression through the diurnal light responses is indicated by the arrowhead symbols and emphasizes the increasing hysteresis under intensifying drought whereby fluxes were suppressed in the afternoons. The four defined periods correspond to the shaded periods in Figure 1 and Table S1.

as a color change (Figure S9). Thus, the high-light, upper canopy environment was relatively inactive physiologically, yet still absorbing substantial solar radiation and acting as a shade (i.e., decreasing LUE), leaving fewer physiologically active leaves in the lower canopy to make use of scant water resources (i.e., increasing iWUE).

4 | DISCUSSION

We used an analogy to the tissue-level PV analysis to determine the whole-ecosystem wilting point, Ψ_{EWP}, using coordinated measurements of Ψ_{pd} and ET. After a plateau, the ecosystem PV curve was characterized by an initial highly sensitive linear decreasing phase followed by a less-sensitive linear one (Figure 2), much like a leaf PV curve that typically has a strongly declining nonlinear phase followed by a less-sensitive linear one (Richter, 1978; Tyree

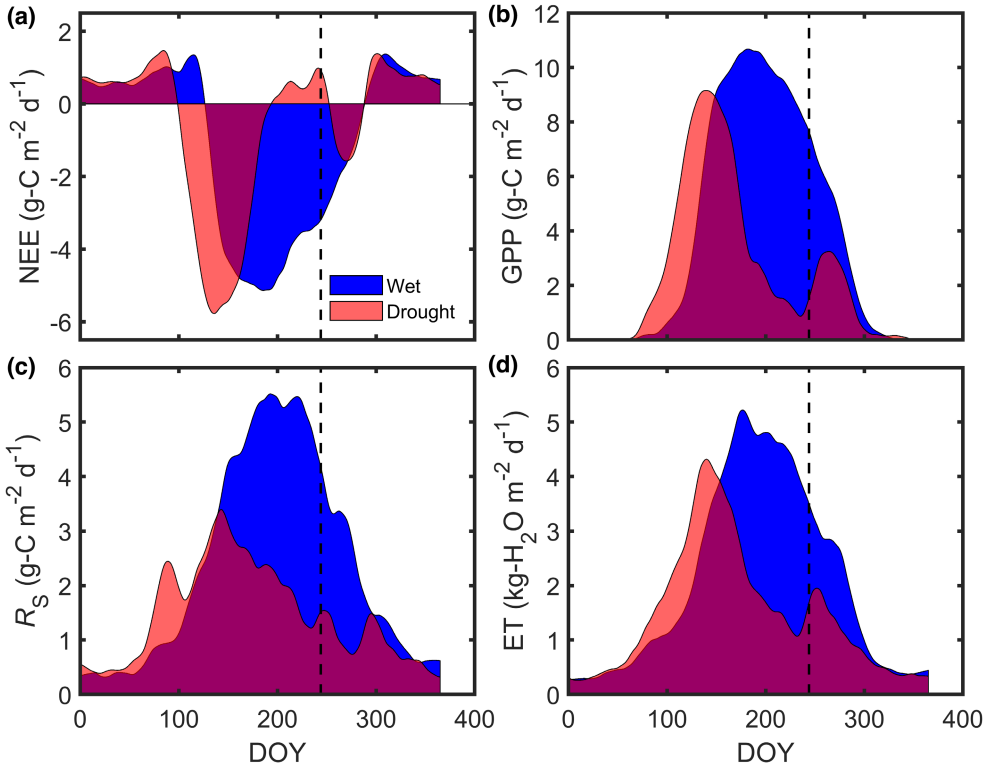

FIGURE 7 Smoothed annual cycles of CO_2 fluxes and evapotranspiration during drought (2012) and wet (mean of 2008 and 2009) years: (a) NEE, net ecosystem CO_2 exchange; (b) GPP, gross primary productivity; (c) R_S, soil respiration; (d) ET, evapotranspiration. The dashed black lines denote the timing of soaking rains.

& Hammel, 1972). This linearization of the initial phase of the ecosystem PV curve was caused by the equilibration of Ψ_{pd} with water in the stem xylem and soil.

We found that the ecosystem wilting point is determined mainly by the ability of roots to acquire water from the drying soil, which, in turn, depends on the rooting profile and soil moisture characteristic curves. Indeed, our bottom-up calculation, based on analysis of the soil moisture characteristic curves and root density distribution, yielded a trait-based "bottom-up" $\Psi_{EWP,soil}$ of −2.0 (−3.12, −1.16) MPa (Figure 3). This was identical to our "top-down" Ψ_{EWP} estimate of −2.0 (−2.23, −1.78) from ecosystem PV analysis (Figure 2), implying that the vegetation has largely coordinated leaf wilting with soil water extraction capacity.

At the Ψ_{EWP}, soil water in the rooting zone is difficult to extract because it is more tightly bound to the soil matrix, and leaves are at or near their turgor loss point. This *Quercus-Carya* forest has relatively thin soils that can be readily exhausted of plant-available water if not replenished by rainfall (Gu, Pallardy, Hosman, et al., 2016), and the Ψ_{EWP} of −2.0 MPa is at or near Ψ_{tlp} for tree species in this forest, which range from −2.0 to −2.7 MPa (Bahari et al., 1985; Parker et al., 1982), and for which the community-weighted mean Ψ_{tlp} is −2.5 MPa.

As an ecosystem trait, Ψ_{EWP}, defines broad shifts in whole-forest behavior. When Ψ_{pd} is below Ψ_{EWP}, but above the leaf Ψ_{tlp} of constituent species, there is still capacity for stomatal opening and gas exchange in the mornings when temperature and VPD are lower and after whatever overnight recovery was possible (Figure 6 and Figure S6). During this time, leaves are subject to diurnal wilting given the sharp downregulation of flux magnitudes by mid-day, that is, aside from the morning, Ψ_{leaf} spends much of the rest day below Ψ_{tlp}. When Ψ_{pd} falls below leaf Ψ_{tlp}, there is turgor loss over the entire day, and the rates of CO_2 and water vapor diffusion through stomata, as well as the transport rates of both gases across the cuticle are highly restricted, but more so for CO_2 (Boyer, 2015).

Incorporating realistic representation of ecosystem wilting is likely to improve the performance of ecosystem models with respect to drought responses. The results of our bottom-up findings underscore the importance of belowground capacity for water extraction, which depends on moisture release characteristics and knowledge of root density profiles and traits (Warren et al., 2015). Furthermore, the evaluation of models in ecosystem functional space (i.e., comparing modeled and observed environmental responses) has proven to be more insightful than the routine 1:1 plots (Gu, Pallardy, Yang, et al., 2016). Validating whether models reproduce data-derived Ψ_{EWP} and associated threshold in ecosystem functional state represents a new avenue for evaluating drought response simulations.

This *Quercus-Carya* forest is highly dependent on new rainfall inputs to replenish the soil water supply during the growing season. Growing season precipitation variability explains most of the considerable interannual variation in plant water stress (Gu, Pallardy, Hosman, et al., 2016), which, in turn, plays a major role in modulating

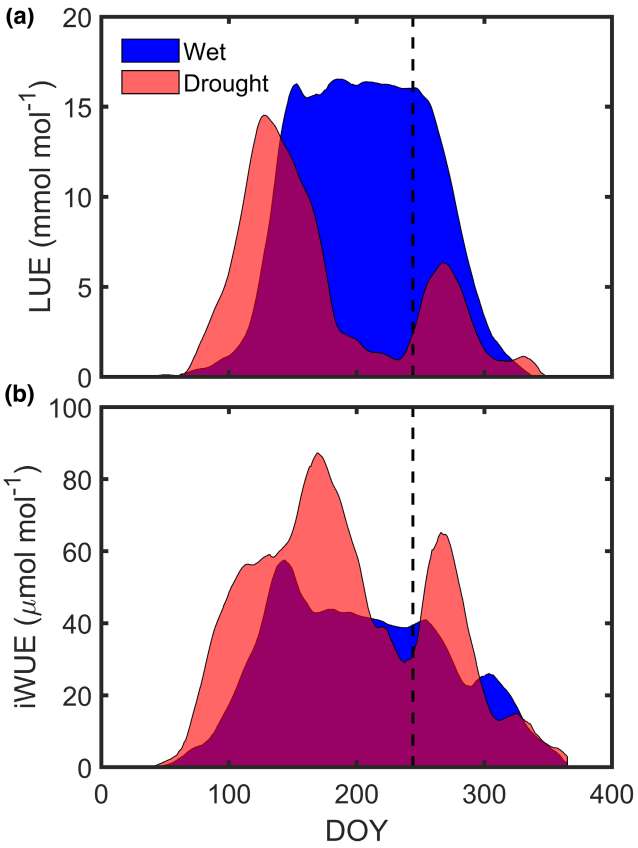

FIGURE 8 Smoothed annual cycles of (a) light-use efficiency (LUE) and (b) ecosystem intrinsic water-use efficiency (iWUE) during drought (2012) and wet (mean of 2008 and 2009) years. LUE and iWUE represent mid-day mean values for conditions of high light (solar irradiance >500 W m^{-2}). The dashed black lines denote the timing of soaking rains.

seasonal and annual gas exchange (Gu, Pallardy, Yang, et al., 2016), as well as drought-induced tree mortality (Gu et al., 2015; Wood et al., 2018). Moreover, there is evidence that early shifts in phenology and productivity place the forest at greater risk of physiological water stress later in the growing season because the depletion of soil water supply begins sooner (He et al., 2020). Over 16 years, this forest functioned below Ψ_{EWP} only ~10% of the time. However, ~60% of Ψ_{pd} observations were below −0.5 MPa (Figure 4), a threshold at which the forest is within 2–4 weeks of entering into rapid intensification of drought stress and/or reaching Ψ_{EWP} in the absence of rainfall (Figures 1b and 5a). Were these times so short because of low plant available soil water going into the growing season? We checked the standardized precipitation evapotranspiration index (SPEI; Beguería et al., 2014), values for our location (retrieved from https://spei.csic.es/database.html). In April 2012, SPEI values (for 1-, 3-, 6-, 12-, and 24-month periods) ranged from +0.48 to +1.6, supporting the generalization of our observations (at least for this site), and that there was not strong antecedent dryness that manifested anomalous behavior in the major 2012 drought year.

As an emergent ecosystem functional property (He et al., 2019; Reichstein et al., 2014), Ψ_{EWP} integrates plant functional responses across the SPAC, linking leaf wilting with capacity for soil water extraction. Our top-down and bottom-up analyses imply that beyond climate, plants coordinate leaf Ψ_{tlp} with their capacity to acquire water from soils. Capacity for water extraction is determined by structural and functional root traits, as well as the soil moisture characteristic (Warren et al., 2015). Leaf Ψ_{tlp} and its plasticity are correlated with climate, and these traits are strong predictors of plant drought tolerance (Bartlett et al., 2012, 2014). Indeed, seasonal osmotic adjustment has been observed in *Quercus* individuals that dominate this forest (Parker et al., 1982). Our top-down conceptualization of Ψ_{EWP} also integrates temporal aspects of tissue water relations, capturing seasonal osmotic adjustment if it occurs.

It is advantageous for plants to coordinate leaf wilting with their ability to extract water from the soil to protect costlier stem tissues (Rodriguez-Dominguez & Brodribb, 2020). Indeed, we found that when Ψ_{pd} falls below Ψ_{EWP}, there is a fundamental shift in functional state whereby responses of ecosystem gas exchange to environmental variations are strongly diminished (Figure 6 and Figures S6 and S8). Conceptually, when there are diminishing returns on soil water extraction, then the leaves should wilt to protect stem tissues from embolism (Martin-St Paul et al., 2017). This may help to explain divergence from the broad patterns of Ψ_{tlp} correlation with water availability determined by climatic water balance in dryland plants (Farrell et al., 2017).

We found that the Ψ_{EWP} is a reversible threshold, finding rapid recovery of ecosystem function after soaking rains, even though Ψ_{pd} had been below Ψ_{EWP} for more than 2 months and reached a seasonal minimum of −3.8 MPa. The rapid leaf rehydration clearly indicates the absence of catastrophic hydraulic disconnection between roots and leaves (Gu et al., 2015). Though NEE recovered to values in-line with wet year conditions, this was not so for GPP, ET, and R_S, all of which were substantially lower in the drought versus wet year at the same time (Figure 7). The more muted GPP recovery can be attributed to drought legacy effects that resulted in decreased photosynthetic capacity, as evidenced by light response curves that showed lower light-saturated GPP during the recovery period relative to the same time during wet years (Figure 6 vs. Figure S7), which was likely caused by a combination of structural and physiological damage. This underscores the divergent paths to the same NEE because of how GPP and respiratory fluxes are correlated (Baldocchi & Sturtevant, 2015) and respond differentially to environmental stresses (Ingrisch & Bahn, 2018). Thus, a key insight is that the drought legacy constrained GPP, but so too was respiration. Finally, it is noteworthy that even though we observed significant impacts during drought, the forest was still a large C sink on an annual basis (NEE = −195 g-C m^{-2}) largely owing to enhanced early spring uptake, which is approximately half of the net annual CO_2 uptake of the wet years (NEE = −390 g-C m^{-2}).

Differential recovery dynamics among physiological processes is common after severe water and heat stress (Ruehr et al., 2019). Rapid recovery, though not necessarily to pre-drought levels, has been observed in terms of leaf rehydration (Bahari et al., 1985; Choat et al., 2018; Galle et al., 2007; Gu et al., 2015; Lempereur et al., 2015; Parker et al., 1982; Skelton et al., 2017), total plant hydraulic

conductance (Anderegg et al., 2014; Skelton et al., 2017), stomatal conductance (Galle et al., 2007; Miyashita et al., 2005), transpiration (Gleason et al., 2017; Miyashita et al., 2005), leaf net photosynthesis (Galle et al., 2007; Miyashita et al., 2005), and forest NEE (Lempereur et al., 2015). In our case, we did not expect functional recovery to a pre-drought state because it was later in the growing season, nearing senescence with decreasing daily PAR totals and temperatures, which together constrain the achievable productivity (Table S1).

LUE and iWUE dynamics shed further light on the impact of the drought legacy on ecosystem function during recovery. Whereas LUE in the drought year was lower than for wet conditions, the opposite was true for iWUE (Figure 8). Notwithstanding the striking plant rehydration during the recovery phase, maximal Ψ_{pd} during recovery was −0.7 MPa, likely constrained by loss of rehydration capacity (John et al., 2018), indicating that the forest was still experiencing water stress. The ecosystem was thus still in water conservation mode with stomata partially closed to increase water-use efficiency (Yang et al., 2021). Such water conservation through partial stomatal closure necessarily reduces LUE, which declines if there is any downregulation of photosynthesis. Second, there was observed damage to the canopy, whereby much of the upper sunlit layer was scorched during the drought. In addition to drought-induced leaf abscission (Figure S3f), which can protect the xylem of more costly woody tissues (Nadal-Sala et al., 2021; Sabot et al., 2022), a considerable amount of necrotic leaf tissue remained intact in the upper sunlit canopy (Kravitz et al., 2016). Thus, large quantities of light would have been absorbed by physiologically inactive leaves, thereby limiting LUE recovery. In contrast, iWUE was amplified because there were fewer physiologically active leaves to make use of scant water resources (Parker & Pallardy, 1985). Clearly post-drought recovery is complicated and, if to be represented accurately in Earth system models, must be vertically resolved to accurately represent reversible physiological processes, irreversible canopy structural changes, and their dynamic interactions.

Our top-down approach to Ψ_{EWP} estimation could also be applied to derive whole-plant wilting points from coordinated sap flux and Ψ_{pd} measurements in either field or greenhouse experiments. This would contribute to improved understanding of dynamic hydraulic coordination among plant organs, and how soils and the rhizosphere influence aboveground plant hydraulic traits (McCulloh et al., 2019). Such whole-plant studies are more conducive to experimental drought treatments, and thus not reliant on natural drydowns, which if they do not occur with sufficient intensity (across the entire root zone), limits the ability to conduct the top-down PV analysis. With further validation, bottom-up scaling approaches that consider key plant traits and soil characteristics would provide an important means of estimating Ψ_{EWP} of ecosystems that do not experience drought at a sufficient intensity. For example, during the 2012 drought, at a more mesic deciduous forest in Indiana, there was marked downregulation of net CO_2 exchange, but the C sink remained intact throughout the drought, and their mid-day Ψ_{leaf} observations were less negative (Roman et al., 2015; Yi et al., 2017) than our predawn Ψ_{leaf} measurements at MOFLUX.

It is clear that greater emphasis on how plants interact with the belowground environment (Warren et al., 2015), and considering the entire critical zone from aquifers to treetop is needed (Dawson et al., 2020) to develop accurate predictions of ecosystem responses to climate change. Tree roots may delve deep enough below the surface to reach aquifers (Jackson et al., 2000; Miller et al., 2010), which can backstop water availability during exceptionally dry conditions to sustain the ecosystem (Baldocchi et al., 2021; Ciruzzi & Loheide II, 2021; Domec et al., 2010; Montaldo & Oren, 2022).

If vegetation has access to groundwater, would the Ψ_{EWP} concept apply? Wilting is a broad, generalized response governed by plant water balances (Bartlett et al., 2014; Tyree & Hammel, 1972). When enough water is lost from a plant, and the water supply (*from whatever source*) to leaves cannot match demand, cells lose turgor pressure and wilt (Bartlett et al., 2016; Kramer, 1950). In theory, the ecosystem wilting point should be similarly generalizable, and the question is, what plant traits and site characteristics define it?

We tested and found support for the hypothesis that the ability of the vegetation to access water defines the ecosystem wilting point for this *Quercus-Carya* forest. At this site, soils are relatively thin and precipitation variability explains a large fraction of interannual variation of species- and community-level water stress (Gu, Pallardy, Hosman, et al., 2016), which, in turn, has a strong effect on tree mortality (Gu et al., 2015) and ecosystem gas exchange (Gu, Pallardy, Yang, et al., 2016). We thus hypothesized that the soil moisture release characteristics across the root zone, which generally is not accessing groundwater, defines the capacity of the forest to extract water. We found that our bottom-up and top-down estimates of whole-ecosystem wilting were in excellent agreement (Figures 2 and 3).

When roots extend down into groundwater, vegetation has a water subsidy to draw upon as a backstop against dehydration during periods with low precipitation (Baldocchi et al., 2021; Chitra-Tarak et al., 2021; Ciruzzi & Loheide II, 2021; Domec et al., 2010; Montaldo & Oren, 2022). Yet, if the water table drops enough (naturally by drought or through management), eventually the ability to access water is diminished and wilting can occur (Miller et al., 2010). Similarly for the case of vegetation that makes use of stored water, eventually there would come a point at which there is insufficient water available to maintain leaf turgor. In both cases, the traits and characteristics defining the ecosystem wilting point would most likely differ from our system. More research across many sites with detailed knowledge of the belowground characteristics and hydrology, and plant structural and functional traits is needed to address these questions more fully.

Achieving step-changes in scientific understanding and process modeling of ecosystem drought response and recovery, especially in the face of global environmental change, demands greater efforts to characterize both the belowground environment and the actual water status of plants (Novick et al., 2022; Paschalis et al., 2020). Knowledge of root system architecture should inform subsurface sensor deployment and/or be used to help interpret data. Pressure chamber measurements of Ψ_{pd} are a simple and straightforward way to gain rich information on the physiological state of the plants (Gu et al., 2015; Gu, Pallardy, Hosman, et al., 2016; Pallardy et al., 1991), and weekly to

bi-weekly measurements are able to characterize rapid ecosystem dry-downs. Even if there is disequilibrium between Ψ_{pd} and the soil water potential (Donovan et al., 2001), knowledge of the former directly quantifies the state of water in the plant, and informs on the level of water stress and how plants are interacting with soil water supply.

We found that Ψ_{EWP} provides integrated information on ecosystem functioning across the SPAC and has a clear physiological link with the dynamics of ecosystem CO_2 and water vapor fluxes. Bottom-up analysis points to the capacity for water extraction, as determined by the root density distribution and soil moisture characteristic curves as being important determinants of Ψ_{EWP}, although more detailed analyses incorporating root functional traits are warranted. Our observations imply that leaf Ψ_{tlp} is coordinated with soil texture and the associated constraints on the soil moisture characteristic. Thus, we hypothesize that Ψ_{EWP} represents a constraint on the plants that can recruit into, survive, and regenerate in the ecosystem, and has great potential for illuminating both the dynamics of ecosystem fluxes and the biogeographic patterns of ecosystem drought adaptation.

ACKNOWLEDGMENTS

The authors gratefully acknowledge the contributions of Dr. Stephen Pallardy and Mr. Kevin Hosman to MOFLUX and their role in collecting the data used in this paper. This material is based upon work supported by the U.S. Department of Energy, Office of Science, Office of Biological and Environmental Research Program, Climate and Environmental Sciences Division through Oak Ridge National Laboratory's Terrestrial Ecosystem Science—Science Focus Area and National Science Foundation grant 2017949. ORNL is managed by UT-Battelle, LLC, for the U.S. Department of Energy under contract DE-AC05-00OR22725.

CONFLICT OF INTEREST

The authors declare no conflict of interest.

DATA AVAILABILITY STATEMENT

Ecosystem flux data are available at: https://ameriflux.lbl.gov/ (site ID, US-MOz). Predawn leaf water potential data (Pallardy et al., 2018) are available at: https://tes-sfa.ornl.gov/node/80. Leaf area index and soil water retention curve data are available at: https://zenodo.org/record/7477879#.Y6XimhXMJPY.

ORCID

Jeffrey D. Wood https://orcid.org/0000-0001-6422-2882
Lianhong Gu https://orcid.org/0000-0001-5756-8738
Paul J. Hanson https://orcid.org/0000-0001-7293-3561
Christian Frankenberg https://orcid.org/0000-0002-0546-5857
Lawren Sack https://orcid.org/0000-0002-7009-7202

REFERENCES

Abrams, M. D., & Menges, E. S. (1992). Leaf ageing and plateau effects on seasonal pressure-volume relationships in three sclerophyllous *Quercus* species in South-Eastern USA. *Functional Ecology*, *6*(3), 353–360.

Anderegg, W. R. L., Anderegg, L. D. L., Berry, J. A., & Field, C. B. (2014). Loss of whole-tree hydraulic conductance during severe drought and multi-year forest die-off. *Oecologia*, *175*(1), 11–23. https://doi.org/10.1007/s00442-013-2875-5

Anderegg, W. R. L., Konings, A. G., Trugman, A. T., Yu, K., Bowling, D. R., Gabbitas, R., Karp, D. S., Pacala, S., Sperry, J. S., Sulman, B. N., & Zenes, N. (2018). Hydraulic diversity of forests regulates resilience during drought. *Nature*, *561*, 538–541. https://doi.org/10.1038/s41586-018-0539-7

Bahari, Z. A., Pallardy, S. G., & Parker, W. C. (1985). Photosynthesis, water relations, and drought adaptation in six woody species of oak-hickory forests in Central Missouri. *Forest Science*, *31*(3), 557–569.

Baldocchi, D. D. (2020). How eddy covariance flux measurements have contributed to our understanding of global change biology. *Global Change Biology*, *26*(1), 242–260. https://doi.org/10.1111/gcb.14807

Baldocchi, D., Ma, S., & Verfaillie, J. (2021). On the inter- and intra-annual variability of ecosystem evapotranspiration and water use efficiency of an oak savanna and annual grassland subjected to booms and busts in rainfall. *Global Change Biology*, *27*(2), 359–375. https://doi.org/10.1111/gcb.15414

Baldocchi, D., & Sturtevant, C. (2015). Does day and night sampling reduce spurious correlation between canopy photosynthesis and ecosystem respiration? *Agricultural and Forest Meteorology*, *207*, 117–126. https://doi.org/10.1016/j.agrformet.2015.03.010

Bartlett, M. K., Klein, T., Jansen, S., Choat, B., & Sack, L. (2016). The correlations and sequence of plant stomatal, hydraulic, and wilting responses to drought. *Proceedings of the National Academy of Sciences of the United States of America*, *113*(46), 13098–13103. https://doi.org/10.1073/pnas.1604088113

Bartlett, M. K., Scoffoni, C., & Sack, L. (2012). The determinants of leaf turgor loss point and prediction of drought tolerance of species and biomes: A global meta-analysis. *Ecology Letters*, *15*, 393–405. https://doi.org/10.1111/j.1461-0248.2012.01751.x

Bartlett, M. K., Zhang, Y., Kreidler, N., Sun, S., Ardy, R., Cao, K., & Sack, L. (2014). Global analysis of plasticity in turgor loss point, a key drought tolerance trait. *Ecology Letters*, *17*(12), 1580–1590. https://doi.org/10.1111/ele.12374

Beguería, S., Vicente-Serrano, S. M., Reig, F., & Latorre, B. (2014). Standardized precipitation evapotranspiration index (SPEI) revisited: Parameter fitting, evapotranspiration models, tools, datasets and drought monitoring. *International Journal of Climatology*, *34*(10), 3001–3023. https://doi.org/10.1002/joc.3887

Boyer, J. S. (2015). Turgor and the transport of CO_2 and water across the cuticle (epidermis) of leaves. *Journal of Experimental Botany*, *66*(9), 2625–2633. https://doi.org/10.1093/jxb/erv065

Briggs, L. J., & Shantz, H. L. (1912). The wiliting coefficient and its indirect determination. *Botanical Gazette*, *53*(1), 20–37.

Cheung, Y. N. S., Tyree, M. T., & Dainty, J. (1975). Water relations parameters on single leaves obtained in a pressure bomb and some ecological interpretations. *Canadian Journal of Botany*, *53*(13), 1342–1346. https://doi.org/10.1139/b75-162

Chitra-Tarak, R., Xu, C., Aguilar, S., Anderson-Teixeira, K. J., Chambers, J., Detto, M., Faybishenko, B., Fisher, R. A., Knox, R. G., Koven, C. D., Kueppers, L. M., Kunert, N., Kupers, S. J., McDowell, N. G., Newman, B. D., Paton, S. R., Perez, R., Ruiz, L., Sack, L., … McMahon, S. M. (2021). Hydraulically-vulnerable trees survive on deep-water access during droughts in a tropical forest. *New Phytologist*, *231*, 1798–1813. https://doi.org/10.1111/nph.17464

Choat, B., Nolf, M., Lopez, R., Peters, J. M. R., Creek, D., & Brodribb, T. J. (2018). Non-invasive imaging shows no evidence of embolism repair after drought in tree species of two genera. *Tree Physiology*, *39*, 113–121. https://doi.org/10.1093/treephys/tpy093

Ciruzzi, D. M., & Loheide, S. P., II. (2021). Groundwater subsidizes tree growth and transpiration in sandy humid forests. *Ecohydrology*, *14*, e2294. https://doi.org/10.1002/eco.2294

Dawson, T. E., Hahm, W. J., & Crutchfield-Peters, K. (2020). Digging deeper: What the critical zone perspective adds to the study of plant ecophysiology. *New Phytologist*, *226*, 666–671. https://doi.org/10.1111/nph.16410

Domec, J. C., King, J. S., Noormets, A., Treasure, E., Gavazzi, M. J., Sun, G., & McNulty, S. G. (2010). Hydraulic redistribution of soil water by roots affects whole-stand evapotranspiration and net ecosystem carbon exchange. *New Phytologist*, *187*(1), 171–183. https://doi.org/10.1111/j.1469-8137.2010.03245.x

Donovan, L. A., Linton, M. J., & Richards, J. H. (2001). Predawn plant water potential does not necessarily equilibrate with soil water potential under well-watered conditions. *Oecologia*, *129*, 328–335. https://doi.org/10.1007/s004420100738

Falge, E., Baldocchi, D., Olson, R., Anthoni, P., Aubinet, M., Bernhofer, C., Burba, G., Ceulemans, R., Clement, R., Dolman, H., Granier, A., Gross, P., Grünwald, T., Hollinger, D., Jensen, N. O., Katul, G., Keronen, P., Kowalski, A., Lai, C. T., … Wofsy, S. (2001). Gap filling strategies for defensible annual sums of net ecosystem exchange. *Agricultural and Forest Meteorology*, *107*(1), 43–69. https://doi.org/10.1016/S0168-1923(00)00225-2

Farrell, C., Szota, C., & Arndt, S. K. (2017). Does the turgor loss point characterize drought response in dryland plants? *Plant, Cell & Environment*, *40*(8), 1500–1511. https://doi.org/10.1111/pce.12948

Flo, V., Martínez-Vilalta, J., Mencuccini, M., Granda, V., Anderegg, W. R. L., & Poyatos, R. (2021). Climate and functional traits jointly mediate tree water-use strategies. *New Phytologist*, *231*(2), 617–630. https://doi.org/10.1111/nph.17404

Galle, A., Haldimann, P., & Feller, U. (2007). Photosynthetic performance and water relations in young pubescent oak (*Quercus pubescens*) trees during drought stress and recovery. *New Phytologist*, *174*, 799–810. https://doi.org/10.1111/j.1469-8137.2007.02047.x

Gampe, D., Zscheischler, J., Reichstein, M., O'Sullivan, M., Smith, W. K., Sitch, S., & Buermann, W. (2021). Increasing impact of warm droughts on northern ecosystem productivity over recent decades. *Nature Climate Change*, *11*(9), 772–779. https://doi.org/10.1038/s41558-021-01112-8

Gleason, S. M., Wiggans, D. R., Bliss, C. A., Comas, L. H., Cooper, M., Dejonge, K. C., Young, J. S., & Zhang, H. (2017). Coordinated decline in photosynthesis and hydraulic conductance during drought stress in *Zea mays*. *Flora*, *227*, 1–9. https://doi.org/10.1016/j.flora.2016.11.017

Grossiord, C., Buckley, T. N., Cernusak, L. A., Novick, K. A., Poulter, B., Siegwolf, R. T. W., Sperry, J. S., & McDowell, N. G. (2020). Plant responses to rising vapor pressure deficit. *New Phytologist*, *226*, 1550–1566. https://doi.org/10.1111/nph.16485

Gu, L., Pallardy, S. G., Hosman, K. P., & Sun, Y. (2015). Drought-influenced mortality of tree species with different predawn leaf water dynamics in a decade-long study of a central US forest. *Biogeosciences*, *12*(10), 2831–2845. https://doi.org/10.5194/bg-12-2831-2015

Gu, L., Falge, E., Boden, T., Baldocchi, D. D., Black, T. A., Saleska, S. R., Suni, T., Verma, S., Vesala, T., Wofsy, S. C., & Xu, L. (2005). Objective threshold determination for nighttime eddy flux filtering. *Agricultural and Forest Meteorology*, *128*, 179–197. https://doi.org/10.1016/j.agrformet.2004.11.006

Gu, L., Massman, W. J., Leuning, R., Pallardy, S. G., Meyers, T., Hanson, P. J., Riggs, J. S., Hosman, K. P., & Yang, B. (2012). The fundamental equation of eddy covariance and its application in flux measurements. *Agricultural and Forest Meteorology*, *152*(1), 135–148. https://doi.org/10.1016/j.agrformet.2011.09.014

Gu, L., Pallardy, S. G., Hosman, K. P., & Sun, Y. (2016). Impacts of precipitation variability on plant species and community water stress in a temperate deciduous forest in the central US. *Agricultural and Forest Meteorology*, *217*, 120–136. https://doi.org/10.1016/j.agrformet.2015.11.014

Gu, L., Pallardy, S. G., Yang, B., Hosman, K. P., Mao, J., Ricciuto, D., Shi, X., & Sun, Y. (2016). Testing a land model in ecosystem functional space via a comparison of observed and modeled ecosystem flux responses to precipitation regimes and associated stresses in a central U.S. forest. *Journal of Geophysical Research: Biogeosciences*, *121*(7), 1884–1902. https://doi.org/10.1002/2015JG003302

He, L., Wood, J. D., Sun, Y., Magney, T., Dutta, D., Köhler, P., Zhang, Y., Yin, Y., & Frankenberg, C. (2020). Tracking seasonal and interannual variability in photosynthetic downregulation in response to water stress at a temperate deciduous forest. *Journal of Geophysical Research: Biogeosciences*, *125*(8), 1–23. https://doi.org/10.1029/2018jg005002

He, N., Liu, C., Piao, S., Sack, L., Xu, L., Luo, Y., He, J., Han, X., Zhou, G., Zhou, X., Lin, Y., Yu, Q., Liu, S., Sun, W., Niu, S., Li, S., Zhang, J., & Yu, G. (2019). Ecosystem traits linking functional traits to macroecology. *Trends in Ecology & Evolution*, *34*(3), 200–210. https://doi.org/10.1016/j.tree.2018.11.004

Höfler, K. (1920). Ein Schema für die osmotische Leistung der Pfianzenzelie. *Berichte der Deutschen Botanischen Gesellschaft*, *38*, 288–298.

Ingrisch, J., & Bahn, M. (2018). Towards a comparable quantification of resilience. *Trends in Ecology & Evolution*, *33*, 251–259. https://doi.org/10.1016/j.tree.2018.01.013251

Jackson, R. B., Sperry, J. S., & Dawson, T. E. (2000). Root water uptake and transport: Using physiological processes in global predictions. *Trends in Plant Science*, *5*(11), 482–488. https://doi.org/10.1016/S1360-1385(00)01766-0

John, G. P., Henry, C., & Sack, L. (2018). Leaf rehydration capacity: Associations with other indices of drought tolerance and environment. *Plant, Cell & Environment*, *41*(11), 2638–2653. https://doi.org/10.1111/pce.13390

Kirkham, M. (2005). *Principles of soil and plant water relations* (1st ed.). Academic Press, Elsevier Inc.

Konings, A. G., Saatchi, S. S., Frankenberg, C., Keller, M., Leshyk, V., Anderegg, W. R. L., Humphrey, V., Matheny, A. M., Trugman, A., Sack, L., Agee, E., Barnes, M. L., Binks, O., Cawse-Nicholson, K., Christoffersen, B. O., Entekhabi, D., Gentine, P., Holtzman, N. M., Katul, G. G., … Zuidema, P. A. (2021). Detecting forest response to droughts with global observations of vegetation water content. *Global Change Biology*, *27*(23), 6005–6024. https://doi.org/10.1111/gcb.15872

Kramer, P. J. (1950). Effects of wilting on the subsequent intake of water by plants. *American Journal of Botany*, *37*(4), 280–284.

Kravitz, B., Guenther, A. B., Gu, L., Karl, T., Kaser, L., Pallardy, S. G., Peñuelas, J., Potosnak, M. J., & Seco, R. (2016). A new paradigm of quantifying ecosystem stress through chemical signatures. *Ecosphere*, *7*(11), e01559. https://doi.org/10.1002/ecs2.1559

Kursar, T. A., Engelbrecht, B. M. J., & Tyree, M. T. (2005). A comparison of methods for determining soil water availability in two sites in Panama with similar rainfall but distinct tree communities. *Journal of Tropical Ecology*, *21*(3), 297–305. https://doi.org/10.1017/S0266467405002324

Lansu, E. M., van Heerwaarden, C. C., Stegehuis, A. I., & Teuling, A. J. (2020). Atmospheric aridity and apparent soil moisture drought in European forest during heat waves. *Geophysical Research Letters*, *47*(6), e2020GL087091. https://doi.org/10.1029/2020GL087091

Lempereur, M., Martin-Stpaul, N. K., Damesin, C., Joffre, R., Ourcival, J. M., Rocheteau, A., & Rambal, S. (2015). Growth duration is a better predictor of stem increment than carbon supply in a Mediterranean oak forest: Implications for assessing forest productivity under climate change. *New Phytologist*, *207*(3), 579–590. https://doi.org/10.1111/nph.13400

Liu, L., Gudmundsson, L., Hauser, M., Qin, D., Li, S., & Seneviratne, S. I. (2020). Soil moisture dominates dryness stress on ecosystem production globally. *Nature Communications*, *11*, 4892. https://doi.org/10.1038/s41467-020-18631-1

Liu, X., Liang, J., & Gu, L. (2020). Photosynthetic and environmental regulations of the dynamics of soil respiration in a forest ecosystem

revealed by analyses of decadal time series. *Agricultural and Forest Meteorology*, *282–283*, 107863. https://doi.org/10.1016/j.agrformet.2019.107863

Liu, Y., Konings, A. G., Kennedy, D., & Gentine, P. (2021). Global coordination in plant physiological and rooting strategies in response to water stress. *Global Biogeochemical Cycles*, *35*(7), e2020GB006758. https://doi.org/10.1029/2020GB006758

Liu, Y., Zhou, R., Wen, Z., Khalifa, M., Zheng, C., Ren, H., Zhang, Z., & Wang, Z. (2021). Assessing the impacts of drought on net primary productivity of global land biomes in different climate zones. *Ecological Indicators*, *130*, 108146. https://doi.org/10.1016/j.ecolind.2021.108146

Liu, Y., Holtzman, N. M., & Konings, A. G. (2021). Global ecosystem-scale plant hydraulic traits retrieved using model-data fusion. *Hydrology and Earth System Sciences*, *25*(5), 2399–2417. https://doi.org/10.5194/hess-25-2399-2021

Liu, Y., Kumar, M., Katul, G. G., Feng, X., & Konings, A. G. (2020). Plant hydraulics accentuate atmospheric moisture stress on transpiration. *Nature Climate Change*, *1*, 691–695. https://doi.org/10.1038/s41558-020-0781-5

Lu, Y., Duursma, R. A., Farrior, C. E., Medlyn, B. E., & Feng, X. (2020). Optimal stomatal drought response shaped by competition for water and hydraulic risk can explain plant trait covariation. *New Phytologist*, *225*(3), 1206–1217. https://doi.org/10.1111/nph.16207

Madani, N., Parazoo, N. C., Kimball, J. S., Ballantyne, A. P., Reichle, R. H., Maneta, M., Saatchi, S., Palmer, P. I., Liu, Z., & Tagesson, T. (2020). Recent amplified global gross primary productivity due to temperature increase is offset by reduced productivity due to water constraints. *AGU Advances*, *1*(4), e2020AV000180. https://doi.org/10.1029/2020av000180

Martin-St Paul, N. K., Delzon, S., & Cochard, H. (2017). Plant resistance to drought depends on timely stomatal closure. *Ecology Letters*, *20*, 1437–1447. https://doi.org/10.1111/ele.12851

McCulloh, K. A., Domec, J. C., Johnson, D. M., Smith, D. D., & Meinzer, F. C. (2019). A dynamic yet vulnerable pipeline: Integration and coordination of hydraulic traits across whole plants. *Plant, Cell & Environment*, *42*(10), 2789–2807. https://doi.org/10.1111/pce.13607

Miller, G. R., Chen, X., Rubin, Y., Ma, S., & Baldocchi, D. D. (2010). Groundwater uptake by woody vegetation in a semiarid oak savanna. *Water Resources Research*, *46*, W10503. https://doi.org/10.1029/2009WR008902

Miyashita, K., Tanakamaru, S., Maitani, T., & Kimura, K. (2005). Recovery responses of photosynthesis, transpiration, and stomatal conductance in kidney bean following drought stress. *Environmental and Experimental Botany*, *53*(2), 205–214. https://doi.org/10.1016/j.envexpbot.2004.03.015

Montaldo, N., & Oren, R. (2022). Rhizosphere water content drives hydraulic redistribution: Implications of pore-scale heterogeneity to modeling diurnal transpiration in water-limited ecosystems. *Agricultural and Forest Meteorology*, *312*, 108720. https://doi.org/10.1016/j.agrformet.2021.108720

Monteith, J. L., & Unsworth, M. H. (1990). *Principles of environmental physics* (1st ed.). Edward Arnold.

Myers, B. J. (1988). Water stress integral—A link between short-term stress and long-term growth. *Tree Physiology*, *4*(4), 315–323. https://doi.org/10.1093/treephys/4.4.315

Nadal-Sala, D., Grote, R., Birami, B., Knüver, T., Rehschuh, R., Schwarz, S., & Ruehr, N. K. (2021). Leaf shedding and non-stomatal limitations of photosynthesis mitigate hydraulic conductance losses in scots pine saplings during severe drought stress. *Frontiers in Plant Science*, *12*, 715127. https://doi.org/10.3389/fpls.2021.715127

Novick, K. A., Ficklin, D. L., Baldocchi, D., Davis, K. J., Ghezzehei, T. A., Konings, A. G., Macbean, N., Raoult, N., Scott, R. L., Shi, Y., Sulman, B. N., & Wood, J. D. (2022). Confronting the water potential information gap. *Nature Geoscience*, *15*, 158–164. https://doi.org/10.1038/s41561-022-00909-2

Novick, K. A., Ficklin, D. L., Stoy, P. C., Williams, C. A., Bohrer, G., Oishi, A. C., Papuga, S. A., Blanken, P. D., Noormets, A., Sulman, B. N., Scott, R. L., Wang, L., & Phillips, R. P. (2016). The increasing importance of atmospheric demand for ecosystem water and carbon fluxes. *Nature Climate Change*, *1*, 1–5. https://doi.org/10.1038/nclimate3114

Pallardy, S. G., Gu, L., Wood, J. D., Hosman, K. P., Sun, Y., & Hook, L. (2018). *Predawn leaf water potential of oak-Hickory Forest at Missouri Ozark (MOFLUX) site: 2004–2020, United States*. https://doi.org/10.3334/CDIAC/ORNLSFA.004

Pallardy, S. G., Pereira, J. S., & Parker, W. C. (1991). Measuring the state of water stress in tree systems. In J. P. Lassoie & T. M. Hinckley (Eds.), *Techniques and approaches in Forest tree ecophysiology* (pp. 27–76). CRC Press.

Parker, W. C., & Pallardy, S. G. (1985). Drought-induced leaf abscission and whole-plant drought tolerance of seedlings of seven black walnut families. *Canadian Journal of Forest Research*, *15*, 818–821. https://doi.org/10.1017/CBO9781107415324.004

Parker, W. C., & Pallardy, S. G. (1987). The influence of resaturation method and tissue type on pressure-volume analysis of *Quercus alba* L . seedlings. *Journal of Experimental Botany*, *38*(188), 535–549.

Parker, W. C., Pallardy, S. G., Hinckley, T. M., & Teskey, R. O. (1982). Seasonal changes in tissue water relations of three woody species of the *Quercus-Carya* forest type. *Ecology*, *63*(5), 1259–1267.

Paschalis, A., Fatichi, S., Zscheischler, J., Ciais, P., Bahn, M., Boysen, L., Chang, J., De Kauwe, M., Estiarte, M., Goll, D., Hanson, P. J., Harper, A. B., Hou, E., Kigel, J., Knapp, A. K., Larsen, K. S., Li, W., Lienert, S., Luo, Y., … Zhu, Q. (2020). Rainfall manipulation experiments as simulated by terrestrial biosphere models: Where do we stand? *Global Change Biology*, *3336–3355*, 3336–3355. https://doi.org/10.1111/gcb.15024

Pulwarty, R. S., & Sivakumar, M. V. K. (2014). Information systems in a changing climate: Early warnings and drought risk management. *Weather and Climate Extremes*, *3*, 14–21. https://doi.org/10.1016/j.wace.2014.03.005

Reichstein, M., Bahn, M., Mahecha, M. D., Kattge, J., & Baldocchi, D. D. (2014). Linking plant and ecosystem functional biogeography. *Proceedings of the National Academy of Sciences of the United States of America*, *111*(38), 13697–13702. https://doi.org/10.1073/pnas.1216065111

Richards, L. A., & Weaver, L. R. (1943). Fifteen-atmosphere percentage as related to the permanent wilting percentage. *Soil Science*, *56*(5), 331–338.

Richter, H. (1978). A diagram for the description of water relations in plant cells and organs. *Journal of Experiment*, *29*(112), 1197–1203.

Rodriguez-Dominguez, C. M., & Brodribb, T. J. (2020). Declining root water transport drives stomatal closure in olive under moderate water stress. *New Phytologist*, *225*(1), 126–134. https://doi.org/10.1111/nph.16177

Roman, D. T., Novick, K. A., Brzostek, E. R., Dragoni, D., Rahman, F., & Phillips, R. P. (2015). The role of isohydric and anisohydric species in determining ecosystem-scale response to severe drought. *Oecologia*, *179*, 641–654. https://doi.org/10.1007/s00442-015-3380-9

Ruehr, N. K., Grote, R., Mayr, S., & Arneth, A. (2019). Beyond the extreme: Recovery of carbon and water relations in woody plants following heat and drought stress. *Tree Physiology*, *39*, 1285–1299. https://doi.org/10.1093/treephys/tpz032

Sabot, M. E. B., De Kauwe, M. G., Pitman, A. J., Ellsworth, D. S., Medlyn, B. E., Caldararu, S., Zaehle, S., Crous, K. Y., Gimeno, T. E., Wujeska-Klause, A., Mu, M., & Yang, J. (2022). Predicting resilience through the lens of competing adjustments to vegetation function. *Plant, Cell & Environment*, *45*(9), 2744–2761. https://doi.org/10.1111/pce.14376

Sack, L., John, G. P., & Buckley, T. N. (2018). ABA accumulation in dehydrating leaves is associated with decline in cell volume, not turgor pressure. *Plant Physiology*, *176*(1), 489–493. https://doi.org/10.1104/pp.17.01097

Scholander, P. F., Hammel, H. T., Hemmingsen, E. A., & Bradstreet, E. D. (1964). Hydrostatic pressure and osmotic potential in leavse of mangroves and some other plants. *Proceedings of the National Academy of Sciences of the United States of America*, *52*, 119–125.

Scoffoni, C., Chatelet, D. S., Pasquet-Kok, J., Rawls, M., Donoghue, M. J., Edwards, E. J., & Sack, L. (2016). Hydraulic basis for the evolution of photosynthetic productivity. *Nature Plants*, *2*, 16072. https://doi.org/10.1038/nplants.2016.72

Skelton, R. P., Brodribb, T. J., McAdam, S. A. M., & Mitchell, P. J. (2017). Gas exchange recovery following natural drought is rapid unless limited by loss of leaf hydraulic conductance: Evidence from an evergreen woodland. *New Phytologist*, *215*(4), 1399–1412. https://doi.org/10.1111/nph.14652

Stocker, B. D., Zscheischler, J., Keenan, T. F., Prentice, I. C., Penuelas, J., & Seneviratne, S. I. (2018). Quantifying soil moisture impacts on light use efficiency across biomes. *New Phytologist*, *218*, 1430–1449.

Stocker, B. D., Zscheischler, J., Keenan, T. F., Prentice, I. C., Seneviratne, S. I., & Peñuelas, J. (2019). Drought impacts on terrestrial primary are underestimated by satellite monitoring. *Nature Geoscience*, *12*, 264–270. https://doi.org/10.1038/s41561-019-0318-6

Tolk, J. A. (2003). Soils: Permanent wilting points. In *Encyclopedia of water science* (2nd ed., pp. 927–929). Marcel Dekker Inc.. https://doi.org/10.1081/e-ews2-120010337

Tyree, M. T., & Hammel, H. T. (1972). The measurement of the turgor pressure and the water relations of plants by the pressure-bomb. *Journal of Experimental Botany*, *23*(74), 267–282.

Tyree, M. T., & Zimmermann, M. H. (2002). *Xylem structure and the ascent of sap* (2nd ed.). Springer-Verlag. https://doi.org/10.1007/978-3-662-04931-0_6

Veihmeyer, F. J., & Hendrickson, H. (1928). Soil moisture at permanent wilting of plants. *Plant Physiology*, *3*, 355–357.

Warren, J. M., Hanson, P. J., Iversen, C. M., Kumar, J., Walker, A. P., & Wullschleger, S. D. (2015). Root structural and functional dynamics in terrestrial biosphere models—Evaluation and recommendations. *New Phytologist*, *205*, 59–78. https://doi.org/10.1111/nph.13034

Wiecheteck, L. H., Giarola, N. F. B., de Lima, R. P., Tormena, C. A., Torres, L. C., & de Paula, A. L. (2020). Comparing the classical permanent wilting point concept of soil (−15,000 hPa) to biological wilting of wheat and barley plants under contrasting soil textures. *Agricultural Water Management*, *230*, 105965. https://doi.org/10.1016/j.agwat.2019.105965

Wood, J. D., Knapp, B. O., Muzika, R.-M., Stambaugh, M. C., & Gu, L. (2018). The importance of drought–pathogen interactions in driving oak mortality events in the Ozark border region. *Environmental Research Letters*, *13*, 015004.

Yang, B., Pallardy, S. G., Meyers, T. P., Gu, L. H., Hanson, P. J., Wullschleger, S. D., Heuer, M., Hosman, K. P., Riggs, J. S., & Sluss, D. W. (2010). Environmental controls on water use efficiency during severe drought in an Ozark Forest in Missouri, USA. *Global Change Biology*, *16*(8), 2252–2271. https://doi.org/10.1111/j.1365-2486.2009.02138.x

Yang, Y.-J., Bi, M.-H., Nie, Z.-F., Jiang, H., Liu, X.-D., Fang, X.-W., & Brodribb, T. J. (2021). Evolution of stomatal closure to optimize water-use efficiency in response to dehydration in ferns and seed plants. *New Phytologist*, *230*, 2001–2010. https://doi.org/10.1111/nph.17278

Yi, K., Dragoni, D., Phillips, R. P., Roman, D. T., & Novick, K. A. (2017). Dynamics of stem water uptake among isohydric and anisohydric species experiencing a severe drought. *Tree Physiology*, *37*(10), 1379–1392. https://doi.org/10.1093/treephys/tpw126

Zhang, J., Griffis, T. J., & Baker, J. M. (2006). Using continuous stable isotope measurements to partition net ecosystem CO_2 exchange. *Plant, Cell & Environment*, *29*(4), 483–496. https://doi.org/10.1111/j.1365-3040.2005.01425.x

Zhang, Q., Ficklin, D. L., Manzoni, S., Wang, L., Way, D., Phillips, R. P., & Novick, K. A. (2019). Response of ecosystem intrinsic water use efficiency and gross primary productivity to rising vapor pressure deficit. *Environmental Research Letters*, *14*(7), 74023. https://doi.org/10.1088/1748-9326/ab2603

Zhang, Z., Ju, W., Zhou, Y., & Li, X. (2022). Revisiting the cumulative effects of drought on global gross primary productivity based on new long-term series data (1982–2018). *Global Change Biology*, *28*(11), 3620–3635. https://doi.org/10.1111/gcb.16178

Zhao, T., & Dai, A. (2022). CMIP6 model-projected Hydroclimatic and drought changes and their causes in the twenty-first century. *Journal of Climate*, *35*(3), 897–921. https://doi.org/10.1175/JCLI-D-21-0442.1

SUPPORTING INFORMATION

Additional supporting information can be found online in the Supporting Information section at the end of this article.

How to cite this article: Wood, J. D., Gu, L., Hanson, P. J., Frankenberg, C., & Sack, L. (2023). The ecosystem wilting point defines drought response and recovery of a *Quercus-Carya* forest. *Global Change Biology*, *29*, 2015–2029. https://doi.org/10.1111/gcb.16582